Nanoscale Advances

ROYAL SOCIETY OF CHEMISTRY

MINIREVIEW

View Article Online
View Journal | View Issue

Cite this: *Nanoscale Adv.*, 2021, **3**, 1569

Recent advances in cathode engineering to enable reversible room-temperature aluminium–sulfur batteries

Sungjemmenla, Chhail Bihari Soni and Vipin Kumar *

The rigorous requirements, such as high abundance, cost-effectiveness, and increased storage capacities, pose severe challenges to the existing Li-ion batteries' long-term sustainability. Room-temperature aluminum–sulfur (Al–S) chemistry, in particular, is gaining importance due to its high theoretical energy density (1700 W h kg^{-1}). Al–S battery technology is one of the emerging metal–sulfur candidates that can surpass current Li-ion chemistries. When coupled with sulfur, aluminum metal brings a cheap and energy-rich option to existing battery technologies. Owing to the unique virtues of the Al–S battery, it has garnered increasing interest among scientific communities. Al–S chemistry has been investigated for quite some time, yet the cell performance remained in its infancy, which poses a challenge to this technology's viability. Besides stabilizing the Al metal anode, the most important challenge in the practical development of Al–S batteries is the development of a suitable sulfur cathode material. Owing to the complexity of this multivalent system, numerous factors have been taken into account, but the best sulfur cathode is yet to be identified. A detailed exploration of sulfur cathodes and their implications on the battery performance are discussed in this mini-review article. We present a detailed picture of cathode materials that may serve as the reference guide for developing more practical cathode materials. Also, fundamental principles and challenges encountered in the development of the sulfur cathodes are highlighted. Through the knowledge disseminated in this mini-review, the development in the multivalent post-Li-ion battery can be accelerated. A glimpse of the future outlook on the Al–S battery system with different potential solutions is also discussed.

Received 5th December 2020
Accepted 21st January 2021

DOI: 10.1039/d0na01019g

rsc.li/nanoscale-advances

1. Introduction

In the era of rapid technological development, the demand for portable energy has grown multi-fold in recent years.[1] Among various known energy storage devices, electrochemical energy storage through Li-ion batteries has become increasingly popular.[2–4] However, conventional Li-ion batteries are gradually reaching their performance plateau due to the limited capacity of electrode materials, relatively low energy density, and high cost.[5–8] Nobel laureate Prof. Goodenough highlights the need for a new battery technology that can safely perform tasks, and offer competitive prices and performance with respect to the well-established fossil fuel technologies.[9–11] To meet the high energy demand, alkali metal-based batteries (for instance, lithium–sulfur (Li–S)) attracted enormous attention recently due to its high theoretical energy density of about 2510 W h kg^{-1}.[12–14] Despite the high performance, environmental-friendliness, and low cost of sulfur, the commercialization of alkali-metal-based batteries is plagued seriously by various intrinsic issues, which include the limited specific capacity, low utilization of electrode materials, limited cycling stability, limited rate-performance, and safety concerns due to the flammable electrolyte and metal dendrites.[15–19] Rechargeable batteries with high energy density, environmental-friendliness, and cost-effectiveness are in demand to power the modern society.[20,21]

Unlike the Li or Na metal, aluminum (Al) is relatively stable in various aqueous or non-aqueous liquid media.[22–24] Al is at least 100 times less expensive than Li metal, and its high natural abundance accounts for its cost-effectiveness.[5,25,26] By weight, Al has a storage capacity of 2980 mA h g^{-1}, which is lower than that of Li (3860 mA h g^{-1}). However, due to the higher density of Al,[27] its volumetric storage capacity is substantially greater than the Li metal anode.[21,27–29] Besides being the most abundant metallic element on earth[30,31] and having a safe and environmental benignancy, it has a theoretical gravimetric capacity of 2980 mA h g^{-1}, which is very close to that of lithium. Besides, Al has a negative redox potential, *i.e.*, ~−1.7 V *vs.* SHE, which is more positive than other metals, *viz.*, lithium and sodium, making it relatively safer than those of other alkali metal anodes in rechargeable batteries.[32,33] In the construction of a typical Al–S battery, an aluminum foil with an ultra-smooth surface serves as an anode, and the elemental sulfur mixed with conductive

Centre for Energy Studies, Indian Institute of Technology Delhi, Hauz Khas, New Delhi, 110016, India. E-mail: vkumar@ces.iitd.ac.in

fillers acts as a cathode. The choice of electrolytes can also aid the kinetics of the reaction in a battery. Al has a tendency to form a passivation layer that increases its inertness towards electrolytes.[34,35] Generally, stripping/plating in an Al–S battery can be enhanced with efficiencies greater than 98% using a room temperature non-aqueous electrolyte. Accordingly, non-aqueous ionic liquid (imidazolium salts + aluminium chloride) electrolytes have been utilized due to their high reaction kinetics towards the Al metal surface.[36–38] Chloroaluminate ionic liquids 'are known to be the first generation ionic liquids', owing to their high ionic conductivity and low volatility.[39] Recently, various other aqueous electrolytes have also been investigated, which provide a safer and cost-effective platform for the development of an Al–S battery.[24,40] As an illustration, the anode and cathode electrodes are separated by an [EMIM]Cl/$AlCl_3$-type ionic liquid and glass-fiber separator (Fig. 1). During discharge, the following reactions are expected to take place at the anode and cathode, respectively.

$$2Al + 14AlCl_4^- \rightarrow 8Al_2Cl_7^- + 6e^- \quad (1)$$

$$8Al_2Cl_7^- + 6e^- + 3S \rightarrow Al_2S_3 + 14AlCl_4^- \quad (2)$$

Upon discharge, the electrolyte dissociates to generate an $Al_2Cl_7^-$ species that move towards the sulfur cathode. It then receives electrons to release $AlCl_4^-$ anions in the electrolyte. The kinetics of these reactions is extremely slow due to the tendency of the Al anode to develop a thin passivation layer that limits its reversibility over a while (a few tens of cycles). Room-temperature ionic liquids are demonstrated to promote electrochemical reversibility in Al–S batteries. However, the [EMIM]Cl/$AlCl_3$-type ionic liquid electrolytes are moisture-sensitive and highly corrosive. Hence, they provide additional impediments to the development of a safe and cost-effective Al–S battery.

Given the advantages offered by Al, Al batteries have attracted increasing attention.[28] In combination with the Al metal anode, various cathode materials have been examined to realize a high-energy and highly stable battery system.[41,42] Some examples include graphite,[41,42] vanadium oxides (VO_2,[43] V_2O_5 (ref. 44)), titanium dioxide,[45] and conductive polymers.[46] Although the abovementioned cathode materials have brought obvious advantages, certain disadvantages have been brought by the traditional insertion-type cathode compounds. For instance, the energy density of such batteries fades quickly due to depletion in the electrolyte concentration.[47] Contrary to the traditional liquid electrolytes, ionic liquids are identified to enhance the Al-ion batteries' cycling stability, but at the cost of slow reaction kinetics. This is inevitable due to the substantial size of the chloroaluminate species $[(Al_xCl_y)^-]$ in ionic liquids.[48,49]

2. Sulfur cathode

Besides the conventional intercalation-type cathodes, sulfur, as an emerging conversion-type cathode coupled with Al, provides prospects to tackle these challenges with respect to the intercalation reactions.[50,51] Sulfur is abundant in nature, cost-effective, and environmentally benign. Owing to the extraordinarily high theoretical specific- (1675 mA h g^{-1}) and volumetric- (3459 mA h cm^{-3}) capacities, sulfur as an electrode material provides intriguing prospects in enhancing the energy density, as well as maintains the electrolyte concentration constant when used in Al–S batteries.[51] However, the Al–S batteries' limitations, such as the slow charge transfer kinetics, sluggish reversible reactions, and low compatibility with the electrolyte, remained an obstacle for the commercialization of this chemistry.[31] To address these challenges, we provide a comprehensive insight into sulfur cathodes. This review provides comprehensive studies on the intrinsic and underlying principles of the sulfur cathode and its composites for Al–S batteries. Other cathode materials are also covered in brief to shed light on their basic properties. Through the knowledge disseminated in this mini-review, the development in the multivalent battery can be accelerated. It may pave the way for a practical solution for an efficient Al–S battery. Fig. 2 depicts a detailed framework

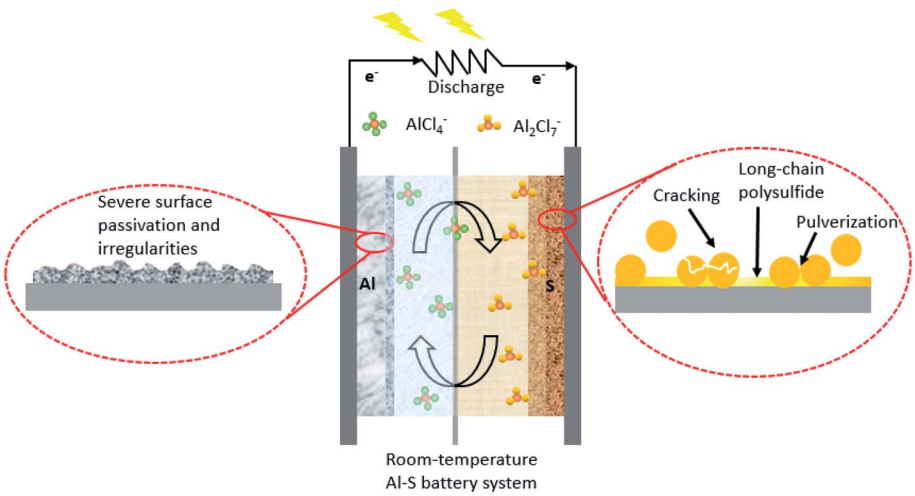

Fig. 1 Schematic representation of the macroscopic and microscopic view of the Al–S battery.

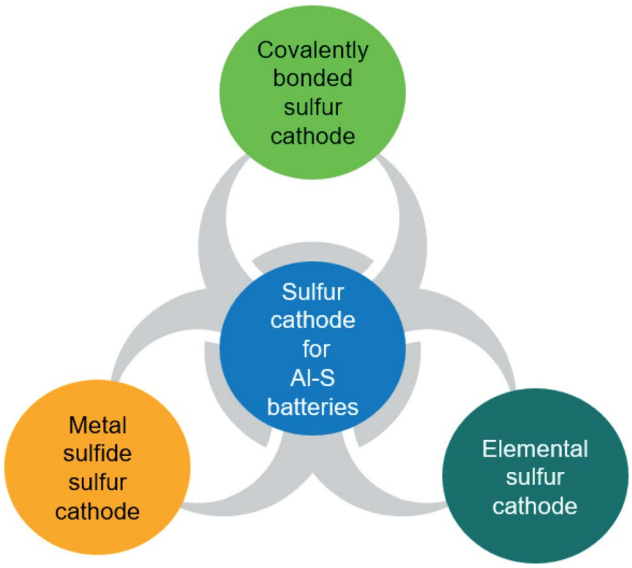

Fig. 2 Schematic illustration of the progress made in the materials chemistry of the cathode to achieve a reversible Al–S battery.

of the progress made in cathode materials for reversible Al–S batteries over time.

2.1. Elemental sulfur/carbon composite for Al–S batteries

With the inception of the interest in Al–S batteries, Licht and co-workers investigated the concentrated polysulfide catholyte and an alkaline aluminium anode for possible application in Al–S batteries.[40] However, the energy densities were about 170 W h kg^{-1} based on dry materials (excluding water) and 110 W h kg^{-1} for the total battery materials with an open-circuit voltage of 1.3 V, which is comparable to that of Li-ion batteries. Likewise, Peramunage *et al.*[52] studied a novel Al–S battery that consists of a concentrated polysulfide catholyte and an alkaline aluminum anode. Among various catholyte solutions, low polarization losses and high storage capacity at the thin-film of CoS were observed for the cathodic polysulfide half-cell of the Al–S battery. An open circuit voltage of up to 1.3 V and specific energy of 110 W h kg^{-1} was achieved for the complete Al–S cell (the theoretical open-circuit voltage of the cell is about −1.8 V, and theoretical specific energy based on potassium salts is about −647 W h kg^{-1}).

The Al–S battery system is a promising platform for realizing high energy density batteries with a scale-up potential with the minimum requirement of the infrastructure, unlike alkali metal–sulfur batteries that require a sophisticated infrastructure for large-scale production. Many efforts have been made to manipulate the battery chemistry to advance this technology. For instance, Cohn *et al.* explored a primary non-aqueous Al–S battery with chloroaluminate ionic liquid as the electrolyte (EMICl/$AlCl_3$).[31] Owing to the high surface area, Ketjen black carbonaceous material was used as the sulfur host for the cathode. This was attributed to the homogeneous dispersion of sulfur particles and strong adhesion with the current collector. The cathode showed a remarkably high specific capacity of more than 1400 mA h g^{-1} (S) at 30 mA g^{-1} (more than 80% of the theoretical capacity of sulfur, *i.e.*, 1675 mA h g^{-1}). However, the capacity of the cell was noticed to fade sharply due to the dissolution of the discharged products, which will affect the rechargeability of the cell. As a result, a relatively low coulombic efficiency was recorded. The specific energy density of about 1700 W h kg^{-1} was estimated based on the first discharge.

Therefore, it is apparent that due to the low charge transfer kinetics, the design and demonstration of a reversible Al–S battery are highly challenging. Gao *et al.*[53] was among the first few to repost a reversible Al–S battery in the presence of an ionic liquid as an electrolyte. Besides the inclusion of an ionic liquid in the cell, the design of the sulfur cathode was also altered. For instance, a microporous carbon coating was employed to block the dissolution of the discharge product. The specific loading of S was estimated to be about 58% in the cathode. The highest specific capacity of about 1230 mA h g^{-1} was obtained at a high current density of 50 mA g^{-1}. Due to the nearly perfect encapsulation of sulfur, an improved reversibility of Al–S could be demonstrated. The microporous carbon with pore size <2 nm was identified to be favorable, leading to an enlarged interfacial area to accommodate the active species,[54,55] thus improving the electron access by reducing the diffusion length for Al^{3+}. As depicted in Fig. 3a, a remarkably high specific capacity of about 1000 mA h g^{-1} (S) was achieved, which leads to a high energy density of 650 W h kg^{-1}. However, the cell could survive only for 20 charges/discharge cycles (Fig. 3b). One of the possible causes of the poor reversibility of the electrochemical reactions in Al–S batteries could lie in the dissociation reaction from $Al_2Cl_7^-$ to free Al^{3+}. Yang *et al.* replaced all $Al_2Cl_7^-$ anions with $Al_2Cl_6Br^-$ anions to alleviate the kinetics of the electrochemical reaction. Owing to the ease of dissociation of the $Al_2Cl_6Br^-$ anions, a high sulfur utilization of about 82% could be obtained using NBMPBr/$AlCl_3$ as the electrolyte. To understand this improvement, DFT calculations were performed, where they evaluated and compared the stability for both $Al_2Cl_6Br^-$ and $Al_2Cl_7^-$ anions. The higher formation energy for $Al_2Cl_6Br^-$ showed a higher stability of these anions. In addition, a smaller LUMO–HOMO gap for $Al_2Cl_6Br^-$ was found to be accountable for its higher dissociation kinetics (at least 15 times) compared to $Al_2Cl_7^-$. This resulted in an initial discharge capacity as high as 1300 mA h g^{-1}, which could maintain over 400 mA h g^{-1} even after 20 cycles.[56] Although non-aqueous electrolytes promote reversibility better than that of aqueous electrolytes, they invite several inevitable issues, such as corrosion and environmental stability. To harness the aqueous electrolytes' benefits, while preserving the reversibility of the redox reactions, water-in-salt electrolytes (such as [Al‖Al(OTF)$_3$ + LiTFSI + HCl‖S/C]) were utilized to demonstrate a rechargeable Al–S battery.[24] They identified that the passivation of the Al anode plays a key role in achieving long-term stability.

The sulfur cathode, which comprises ZIF-67 as the host for sulfur, exhibited an initial specific capacity of 1410 mA h g^{-1} (for sulfur loading of 0.2 mg cm^{-2} only). It retained a reversible capacity of about 420 mA h g^{-1} after 30 cycles at a high current density of 200 mA g^{-1}, and the coulombic efficiency was recorded to be about 97% (Fig. 3c). In addition to the improved

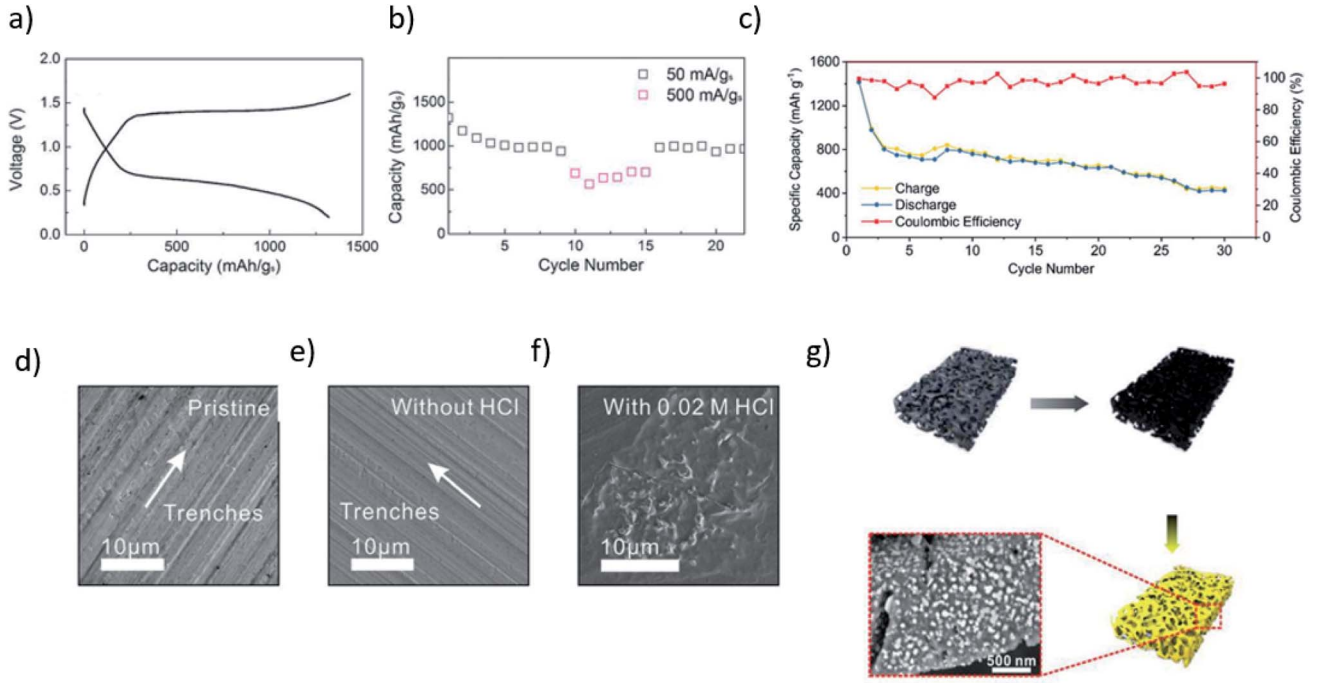

Fig. 3 (a) A typical charge/discharge curve of the Al/S battery at room temperature with the ACC/S cathode, ionic-liquid electrolyte, and the Al foil anode. Current: 50 mA g^{-1}. (b) Cycling stability of the Al/S cell.[53] Reproduced with permission. Copyright 2016 John Wiley and Sons. (c) Discharge and charge capacities, and the coulombic efficiencies as a function of the cycle number for the cell, (d) pristine Al foil, and from Al foils immersion in the (e) electrolyte without HCl, and in (f) the electrolyte containing 0.02 M HCl for 24 h.[24] Reproduced with permission. Copyright 2020 Royal Society of Chemistry. (g) Schematic illustrating the preparation process of S@HKUST-1-C.[57] Reproduced with permission. Copyright 2019 John Wiley and Sons.

reversibility, the cell voltage could be extended to 3.0 V *vs.* Al/Al^{3+} in the presence of water-in-salt electrolytes. Moreover, a trace amount (0.02 M) of HCl additive in the water-in-salt electrolyte inhibits the hydrolysis of AlS_x, and leads to promoting the smooth stripping/plating of the Al metal (Fig. 3f).

Guo and co-workers further improved the stability and reversibility of the charge/discharge reactions in the Al–S battery. They fabricated a metal–organic framework (MOF) derived microporous carbon decorated with Cu nanoparticles (HKUST-1-C) as a possible host for sulfur particles (Fig. 3g). The presence of Cu nanoparticles in the host improves the cathode's performance by eliminating the possibility of polysulfide dissolution. As a result, a high initial discharge capacity of about 1200 mA h g^{-1} could be achieved at a current density of 1000 mA g^{-1}. The S@HKUST-1-C retained a reversible capacity of about 600 mA h g^{-1} and 460 mA h g^{-1} after the 75th and 500th cycles, and the coulombic efficiency was about 90% and 95%, respectively. It has been shown that the presence of the Cu nanoparticles promotes the reversibility of sulfur due to its ability to form an ionic cluster with polysulfide. In addition to that, the conductive character of the Cu nanoparticles significantly minimizes the kinetic barrier during the electrochemical conversion of sulfur.[57]

Xia *et al.* investigated a rechargeable Al–S battery comprising a S–C cathode and dichloromethane (DCM) electrolytes. It could exhibit an initial discharge capacity of 113.64 mA h g^{-1} (pure ionic liquid – 85.23 mA h g^{-1}), which retained its highest value of about 131.67 mA h g^{-1} at the 3rd cycle and 104.69 mA h g^{-1} at the 40th.[39]

In addition to MOF-derived microporous carbon as the host for sulfur particles, a carbon nanofibers (CNF)-based assembly was also examined as the possible host materials for the sulfur cathode. Among the widely studied materials, carbon nanotubes (CNTs)[58–60] and carbon nanofibres (CNFs)[54,61,62] are commonly used carbonaceous cathode materials for lithium–sulfur batteries. They have high conductivity, good mechanical flexibility and strength, large surface area, and a porous structure. For instance, Yu *et al.* coated single-wall carbon nanotubes (SWCNT) on the separator of a reversible room temperature Al–S battery.[63] This, in turn, behaved as a significant barrier to mitigate the diffusion of the polysulfide species, and thereby showed a reduction in the cell's polarization. A freestanding CNF paper as the host for sulfur was also fabricated for the cathode (Fig. 4).

Likewise, Smajic *et al.* designed a composite of sulfur with single-walled carbon nanotubes (SWCNT) as the cathode, and $AlCl_3$·[EMIM] was used as the electrolyte.[50] Besides the improved charge transfer kinetics, the addition of CNTs also improves the Al–S battery capacity with minimal decay per cycle. They unraveled the unique attributes of CNTs that minimize the capacity decay by enhancing the interaction between chloroaluminate ions and sulfur. However, despite the above-mentioned advantages offered by the SWCNT–S cathode, their studies have shown that the formation of short-chain polysulfides could hinder the diffusion of electrons (Fig. 5a),

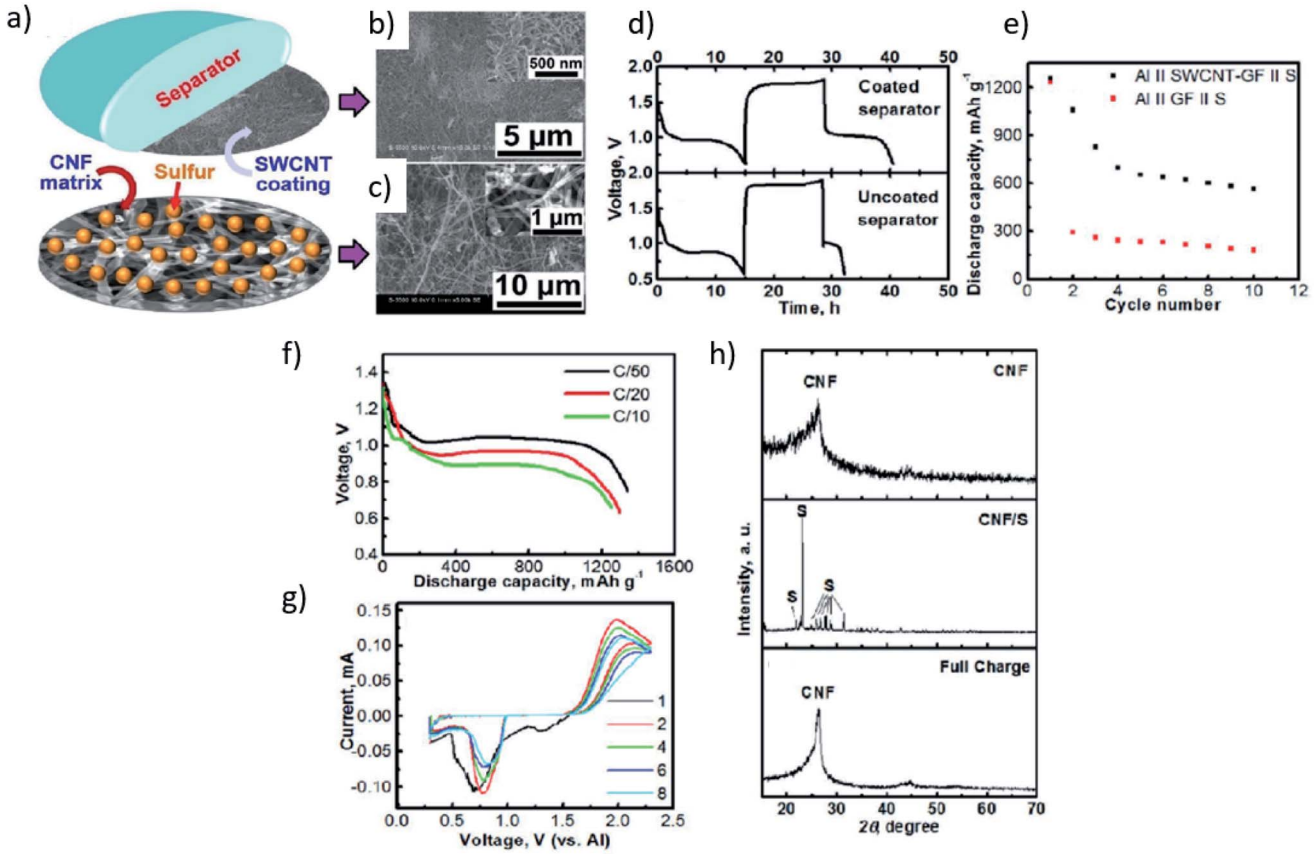

Fig. 4 (a) Schematic of an electrode (cathode)–separator assembly for a non-aqueous room-temperature Al–S battery. (b) Scanning electron microscope (SEM) image of a single-wall carbon nanotube (SWCNT) coating on a glass fiber separator. (c) SEM image of a carbon nanofiber (CNF) matrix. Voltage *versus* time profiles of (d) an Al||SWCNT–GF||S cell (up) and Al||GF||S cell at C/20 rate (down). (e) Discharge capacities as a function of the cycle number of the Al||SWCNT–GF||S and the Al||GF||S cells at the C/20 rate. (f) Voltage profiles of the Al||SWCNT–GF||S cell at various C rates. (g) Cyclic voltammetry profiles (at the first, second, fourth, sixth, and eighth cycle) of the Al||SWCNT–GF||S cell at a scan rate of 0.03 mV s^{-1}. (h) X-ray diffraction (XRD) patterns of a CNF matrix, a fresh CNF/S electrode and a CNF/S electrode upon a discharge–charge cycle, respectively.[48] Reproduced with permission. Copyright 2017 John Wiley and Sons.

resulting in capacity decay. A freestanding CNF paper as the host for a sulfur electrode with Li^+ ions-mediated electrolyte was designed by Yu and his group to promote reversibility in the Al–S battery. With the addition of the Li-ions mediated electrolytes, the cell's performance could be enhanced significantly. For instance, the initial discharge capacity of about 1000 mA h g^{-1} was achieved, and the specific capacity as high as 600 mA h g^{-1} could be retained after 50 cycles (Fig. 5c). The study showed that the Li-ions initiate the chemical reactivation of the Al polysulfide and during cycling (Fig. 5b). Furthermore, the presence of the Li^+ ion in the electrolyte (Al[EMI]Cl_4 ionic liquid) causes the kinetic barrier to become lower by the formation of soluble polysulfide intermediates. It also suppressed the formation of Al═S upon full discharge of the composite sulfur cathode.[49] DFT calculations were performed to understand the thermodynamic behavior of Li_3AlS_3 upon mixing of Li, Al and S atoms, where they have studied the relationship of the relative thermodynamic stability for Li_3AlS_3 and its phase segregated products as expressed in the following eqn (3):

$$Li_3AlS_3 \rightarrow \tfrac{3}{2}Li_2S + \tfrac{1}{2}Al_2S_3 \quad (3)$$

The predicted mixing enthalpy ΔH_{mix} for Li_3AlS_3 showed a positive value of about 0.5 eV. Despite a substantial decrease in ΔH_{mix} and complete miscibility, it could not be achieved for the segregated phases, *i.e.*, Li_2S and AlS_3. This was credited to the amorphization of Li_2S and AlS_3-like phases. It was predicted that upon full discharge of the sulfur cathode, the Li^+ ions mediated electrolyte could enhance the reactivation of the reduced sulfur products by suppressing the formation of the segregated phases, resulting in the improved performance of the Al–S batteries.[49]

2.2 Metal sulfide/carbon composite for the Al–S batteries

The development in the metal–sulfur chemistry is critically impeded by various obstructions related to the sulfur cathode, such as its serious polysulfide solubility, shuttling, and slow kinetics. Massive efforts have been made to investigate other materials systems for the sulfur cathode. Among various known sulfur compounds, the high theoretical specific capacity of transition metal sulfides paves the way for enhancing the chemical stability and ionic/electrical conductivity. For

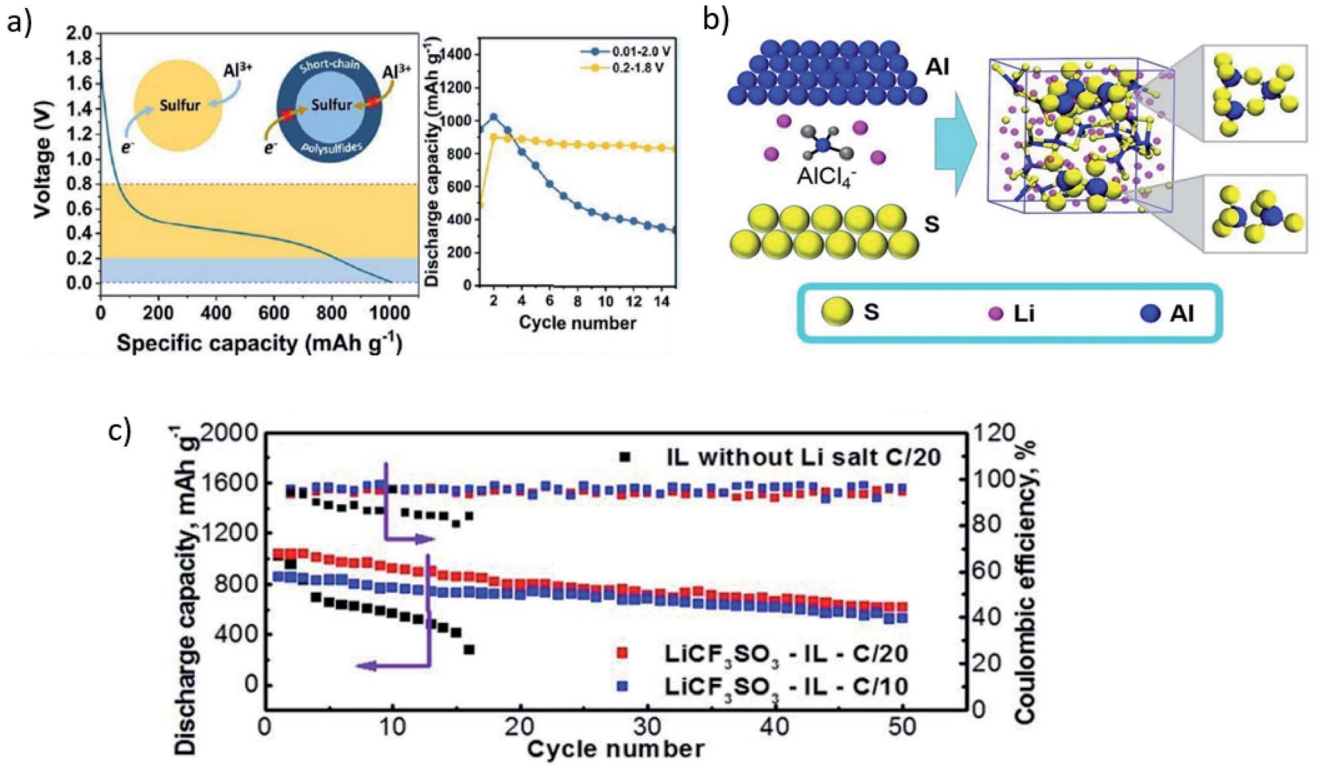

Fig. 5 (a) Voltage profiles of the SWCNT/S cathode (left) and comparison of the SWCNT/S cathode cycling stability with different voltage limits (right).[50] Reproduced with permission. Copyright 2020 American Chemical Society. (b) Schematic representation of the mechanism of the Li-ion mediated IL electrolyte (up). (c) Discharge capacities and coulombic efficiencies as a function of the cycle number for the Al||Li^+–Al[EMI]Cl_4||S cell and the Al||Al[EMI]Cl_4||S cell.[49] Reproduced with permission. Copyright 2018 Elsevier.

example, LiS[64–66] and NaS[67–71] have previously been examined as the potential candidate for the sulfur cathode in metal–sulfur batteries. Although the electronic conductivity of the majority of metal-sulfides is limited[72] – NiS_2 (2–55 S cm^{-1}),[73] TiS_2 (30–50 S cm^{-1}),[74] Co_9S_8 (290 S cm^{-1}),[75] their polar character provides a tremendous binding effect. Hence, this offers a strong chemical interaction to mitigate the polysulfide dissolution or shuttling.[67,76,77] Besides the strong chemical binding with polysulfide, such cathodes offer another significant intrinsic benefit of a substantial sulfiphilic property.[68,78]

The molybdenum sulfide polymorph, such as Mo_6S_8, is one of the oldest known cathode materials that is being examined for various metal anode systems, for instance, Li–S and Mg–S. The unique crystal structure of Mo_6S_8 has stacks of Mo_6S_8 blocks composed of the sulfur anionic cubic cell with an octahedral cluster of Mo atoms. Due to availability of two different types of intercalation sites in Mo_6S_8 structure, it can easily accommodate cations, such as Li^+, Cu^+, and Mg^2.[51,79,80] Inspired by its unique crystal structure, Aurbach and co-workers used Mo_6S_8 as a cathode to demonstrate a rechargeable Mg-ion battery.[81] Geng *et al.* examined the same materials system, *i.e.*, Mo_6S_8, for their possible applications in room-temperature Al–S batteries. The initial discharge capacity of about 40 mA h g^{-1} and 25 mA h g^{-1} at current densities of 60 mA g^{-1} and 120 mA g^{-1}, respectively, could be achieved.[82] The reversibility of the cell for over 50 cycles could be achieved due to the formation of $Al_2Mo_6S_8$ after Al intercalated Mo_6S_8 at two different sites in the crystal lattice. Further investigations are needed towards understanding the Al intercalating and trapping mechanism. Over the past few years, numerous efforts have been made towards various issues encountered by the sulfur cathode for Al–S batteries Wang *et al.* examined metal–sulfur composite materials.[33] A cathode comprising Ni_3S_2/graphene micro flakes was designed for a rechargeable Al-ion battery. The bond length of Ni in the heazlewoodite Ni_3S_2 crystalline structure is 2.50 Å. It shows a trigonal crystal lattice orientation with the *R*32 space group.[83,84] The metal sulfide composite cathode showed an initial discharge capacitance of 350 mA h g^{-1} and a discharge capacity of 60 mA h g^{-1} at the 100th cycle when the current density was 100 mA g^{-1}. A reversible capacity of about 50 mA h g^{-1} could still be achieved at 200 mA g^{-1} after 300 cycles with the coulombic efficiency of about 99% (Fig. 6a and b). Yu *et al.*[86] synthesized hexagonal NiS nanobelts with nickel(II) acetate and sodium thiosulfate as the precursors through a temperature hydrothermal method (Fig. 6c). As illustrated in Fig. 6d, the obtained NiS nanobelts exhibited a specific capacity of about 100 mA h g^{-1} at 200 mA g^{-1} after 100 cycles with good cyclic stability of 90% capacity retention. Fig. 6e shows the performance of the composite cathode up to current densities of 300 mA g^{-1}, exhibiting high cycling stabilities. After 10 cycles, 111.7 mA h g^{-1} discharge capacity was observed at 150 mA g^{-1},

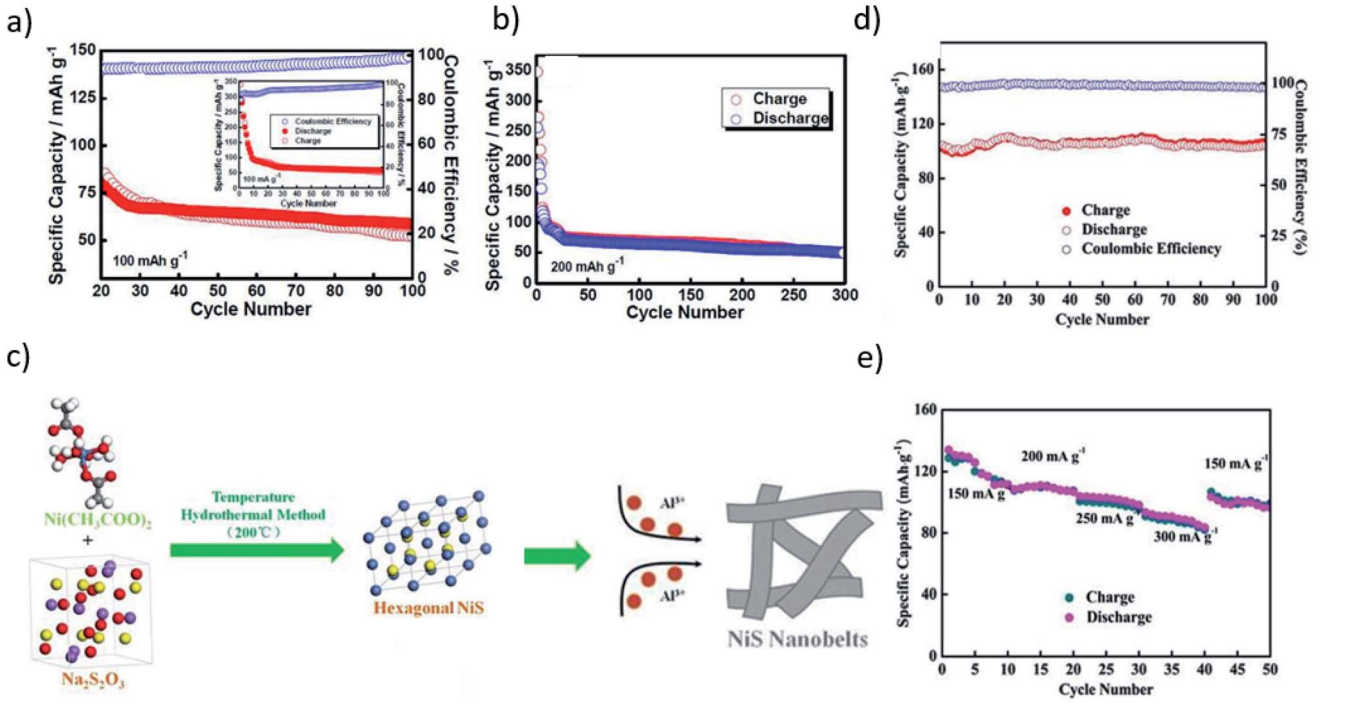

Fig. 6 (a) The cycling performance and the coulombic efficiency at a current density of 100 mA g^{-1}. (b) The cycling performance at a current density of 200 mA g^{-1}.[33] Reproduced with permission. Copyright 2016 John Wiley and Sons. (c) Schematic illustration of the formation process of NiS nanobelts. (d) The cycling performance and the coulombic efficiency at a current density of 200 mA g^{-1}. (e) The rate cycling performances of the NiS nanobelts.[86] Reproduced with permission. Copyright 2016 Royal Society of Chemistry.

which decreased to 83.6 mA h g^{-1} at 300 mA g^{-1} and 96.8 mA h g^{-1} at 150 mA g^{-1}. Although the Al^{3+} diffusion was enhanced, the battery suffered from low voltage plateaus (1.15 V *vs.* Al^{3+}/Al). Unveiling the mechanism of the charge/discharge reactions in sulfur-based cathodes is of great importance. Characterization tools (for instance XRD, TEM and XPS) could offer approximate information about the structural and chemical integrity of the electrode material upon charge/discharge reactions. However, it is utterly complicated to obtain the exact information about the chemical processes due to the inherent limitations of these techniques. Besides that, these techniques suffer from voltage fluctuations or oxidation on exposure to air, which results in inaccurate information. Contrary to the conventional characterization techniques, *in situ* characterization or *operando* methods have become increasingly important, as it has become possible to monitor the instant activities that may occur in the vicinity of the electrode. In addition, such methods provide discernment to the intermediate reactions and corresponding phases. Thus, they can be more precise and reliable. Recently, Li *et al.*[85] evaluated the surface chemistry of the Co_3S_4 electrode upon charge/discharge reaction using *in situ* Raman spectroscopy. Unlike the conventional spectroscopic techniques, *in situ* Raman spectroscopy could unveil the localized concentration variation of the tetrachloroaluminate ions on the surface of the electrode, which possibly could be due to intercalation of the dissociated products of $Al_2Cl_7^-$ into the Co_3S_4 structure during discharge. However, during charging, the ions could not be fully extracted. The Co_3S_4 cathode exhibited an initial discharge capacity of about 287 mA h g^{-1} at a current density of 50 mA g^{-1}, and the cathode retained a capacity of 90 mA h g^{-1} after 150 cycles. The Co_3S_4 cathode exhibited an initial discharge capacity of about 287 mA h g^{-1} at a current density of 50 mA g^{-1}, and the cathode retained a capacity of 90 mA h g^{-1} after 150 cycles.[85]

The Zheng group fabricated a graphene/CoS_2/S composite cathode for a rechargeable Al–S battery.[87] The composite with a high S-content of about 48% led to a high discharge capacity of 1145 mA h g^{-1} for the current density of 50 mA g^{-1} and stable cycle life for over 38 cycles. The surface of the as-fabricated composite sulfur cathode was in direct contact with the rGO-coated separator, which behaved as a barrier to mitigate the diffusion of polysulfides and lowered the polarization. With the addition of a small amount of CoS_2 of ~9 mg cm^{-2} into the composite structure, the enhancement of the polysulfide electrochemical reaction could be expedited due to the strong adsorption sites provided by the CoS_2 particles. Zhang *et al.* prepared 2D layered materials (*e.g.*, MoS_2, WS_2, and BN) as sulfur fixers during repeated charge/discharge processes for achieving high-performance rechargeable Al–S batteries. BN/S/C, when used as the cathode, exhibited the highest capacity of 532 mA h g^{-1} @ 100 mA g^{-1}. In addition, a remarkable life span of up to 300 cycles with a high coulombic efficiency of 94.3% and discharge plateaus at ~1.15 V *vs.* $AlCl_4^-$/Al was displayed for the Al–S battery.[88]

2.3 Covalently bonded sulfur composite for Al–S batteries

As discussed in previous sections, the elemental sulfur cathode or sulfur–carbon composite cathode or metal-sulfide-based

sulfur cathode was found to suffer low discharge capacity and low coulombic efficiency, which are directly related to polysulfide diffusion. A polymeric sulfur host, such as sulfurized polyacrylonitrile (SPAN) has widely been used in Li–S[89–91] and Na–S batteries[92,93] as the cathode due to its strong covalent bonding. PAN constitutes the nitrile group, which on heating with elemental sulfur, gets destabilized to form SPAN. It is a polymeric sulfur composite composed of pyrrolidine rings constituting C=C, C=N, and S–C bonds in the molecular structure of the SPAN composite.[94–96] The electrochemical reactivity of SPAN with monovalent cations is well established with good electronic conductivity of 10^{-4} S cm^{-1}.[97] Wang *et al.* studied the reactivity of the SPAN cathode with Al^{3+}-ions. Owing to the high covalent binding in SPAN, significant control over the high irreversibility of AlS_x could be achieved. Unlike intercalation or conversion type cathode, the S–S bond peaks upon binding of Al^{3+} ions with active sites of S/N atoms, as confirmed by the cyclic voltammograms (CVs) depicted in Fig. 7a. It should be noted that the increase in discharge capacity from 320 mA h g^{-1} to 605 mA h g^{-1} remains at 210 mA h g^{-1} after a subsequent number of cycles (Fig. 7b). Fig. 7c depicts the low voltage plateau (1^{st} discharge cycle) with the low reduction potential curve (1^{st} scan in the cyclic voltammetry curve). The SPAN composite demonstrated high rate capacities of 343, 258, 160, 93 and 54 mA h g^{-1} @ 0.025, 0.05, 0.1, 0.2, and 0.5 A g^{-1}, respectively (see Fig. 7d).[98] Detailed information on the sulfur materials for room-temperature Al–S batteries is summarized in Table 1.

3. Outlook and future perspectives

As summarized in this mini-review, more progress has been made towards the development of a stable sulfur cathode for the long-life and reversible Al–S batteries. The focus has been laid on the latest advances of sulfur cathode components.[99] The positive and negative aspects have been well considered. Research on rechargeable Al–S batteries is booming, and the bottleneck for this battery system can thus be further eliminated. However, owing to the polysulfide shuttling effect of the sulfur electrode and the underlying factors, the Al–S batteries go through complex electrochemical mechanisms rendering their sluggishness in the kinetics of the entire cell. In addition to the conventional challenges encountered by the sulfur cathode, the volumetric strain and the shuttle effect due to the inclusion of Al^{3+} need to be studied in detail. The aim towards high energy density batteries could be achieved by redefining the problems as they claim, "New challenges are redefined under these boundaries regarding low ionic conductivity of high-concentrated Al-PSs electrolyte, saturation and premature precipitation of Al-PSs, and rapid failure of the metal anode". The aforementioned challenges can be mitigated through modifications in the chemical and physical structure of the sulfur cathode. These approaches can be investigated to provide comprehensive knowledge, and applied towards improving the kinetics of Al batteries (Fig. 8).[99]

For example, the inclusion of a core–shell structure has made tremendous progress in lithium and sodium–sulfur battery systems.[91,100] They exhibited stronger physical

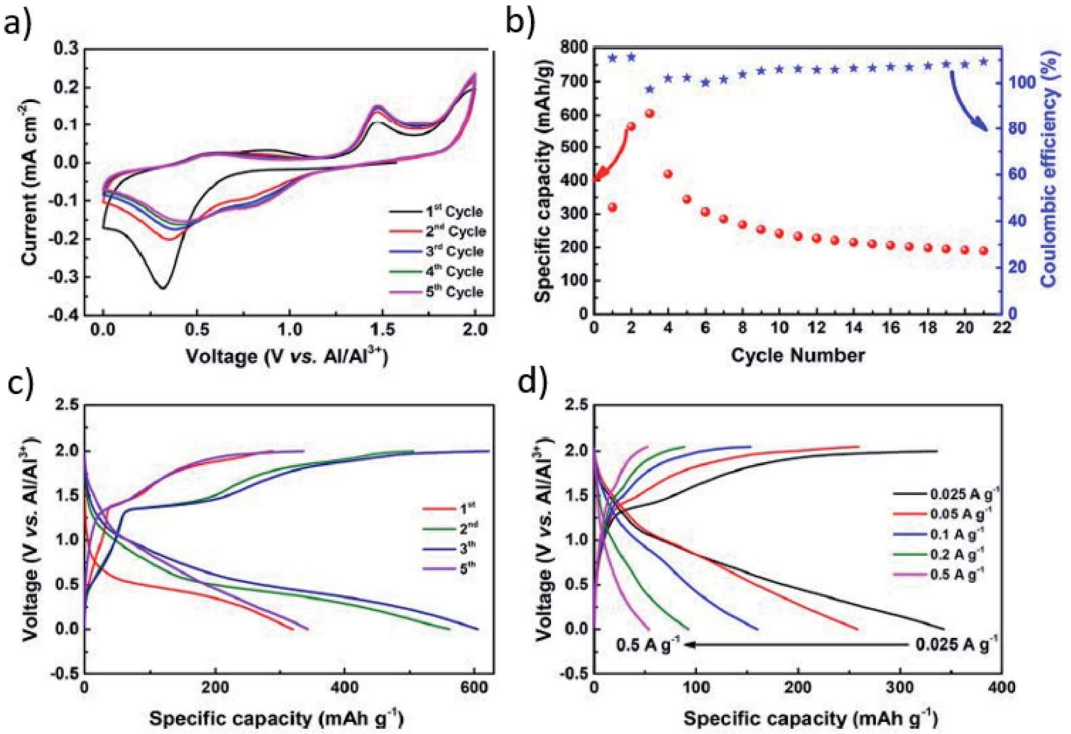

Fig. 7 Electrochemical performance of SPAN in Al–S battery applications. (a) Cyclic voltammograms, (b) cycle performance, (c) galvanostatic (dis-)charge curve, (d) rate capabilities.[98] Reproduced with permission. Copyright 2018 American Chemical Society.

Table 1 Sulfur cathode materials explored for room-temperature Al–S batteries

S. no.	Material system	Synthesis route	Initial discharge capacity (mA h g^{-1})	Discharge (mA h g^{-1}) at ~n cycles	Advantage	Disadvantage
1	Ketjen black carbon/S[31]	Solution-processed slurry based method	1200 @ 120 mA g^{-1}	<50 after 4 cycles	High energy density (1700 W h kg^{-1})	Inability to oxidize AlS_x, fast capacity decay
2	Activated carbon cloth/S[53]	Melt diffusion method	1320 @ 50 mA g^{-1}	1000 @ 20th cycles	Improved reversibility	Large voltage hysteresis, slow solid-state sulfur conversion reaction, and low cycle efficiency (20 cycles)
3	S@CMK-3 (ref. 56)	Melt diffusion method	1390 @ 251 mA g^{-1}	>400 after 20 cycles	Enhanced charge/discharge kinetics and high S-utilisation of 82%	Short cycle life (20 cycles) and polysulfide diffusion
4	Carbonised-ZIF/S[24]	Solvothermal synthesis	1410 @ 200 mA g^{-1}	420 after 30 cycles	Passivation of Al anode and inhibition of hydrolysis of AlS_x	Large voltage hysteresis and low S-loading (0.2 mg cm^{-2})
5	S@HKUST-1-C[57]	Hydrothermal method	1200 @ 1000 mA g^{-1}	460 @ 500th cycles	Improved reversibility and enhanced cycle efficiency	Reduced utilization of sulfur
6	S[39]	Commercial S-powder	113.64 @ 15 mA g^{-1}	104.69 after 40 cycles	Improved performance of the electrolyte	Low discharge capacity and loss of sulfur
7	CNF/S as cathode & SWCNT coated separator[48]	Vacuum filtration and vacuum drying	>1200 @ 0.05C	>450 after 10 cycles	Reduced polarization and alleviate polysulfide diffusion	Low S-loading (1 mg cm^{-2})
8	SWCNT/S[50]	Nondestructive sublimation–deposition method	>900 @ 100 mA g^{-1}	1024 @ 2nd cycle	Improved charge transfer kinetics	Capacity decay
9	CNF/S as cathode & SWCNT-coated GF separator[49]	Vacuum filtration and vacuum drying and activation process	~1000 @ 0.05C	600 after 50 cycles	Enhanced reversibility and suppressed formation of Al═S	Low sulfur-loading (1 mg cm^{-2})
10	Mo_6S_8 (ref. 82)	Chemical intercalation process	148 @ 12 mA g^{-1}	70 after 50 cycles	Good cyclic stability	Low discharge capacity
11	Ni_3S_2/graphene micro flakes[33]	Mixing	350 @ 100 mA g^{-1}	60 after 100 cycles	High discharge voltage plateau (≈1.0 V *vs.* Al/$AlCl_4^-$)	Side reactions due to the dissociation process of complex-ions ($Al_2Cl_7^-$)
12	NiS[86]	Hydrothermal method	104.7 @ 200 mA g^{-1}	100 after 100 cycles	Facilitation of the electrolyte immersion and enhancement of Al^{3+} diffusion, high storage capacity, good cyclability and low overpotential	Low cell voltage plateau (~1.15 V *vs.* Al^{3+}/Al)
13	Graphene/CoS_2/S as cathode & rGO coated separator[87]	Melt diffusion method and hydrothermal method	680 @ 50 mA g^{-1}	1145 after 37 cycles	Suppress polysulfide diffusion and decrease polarisation	Low sulfur loading of 0.2–0.4 mg cm^{-2}
14	SPAN[98]	Thermal polymerization	343 @ 0.025 mA g^{-1}	201 after 20 cycles	Superior rate capacities	Low cycle life and low S-loading (1.5 mg cm^{-2})
15	Co_3S_4 (ref. 85)	Solvothermal process	287.9 @ 50 mA g^{-1}	90 after 150 cycles	Good rate performance	Rapid capacity loss and limited current density

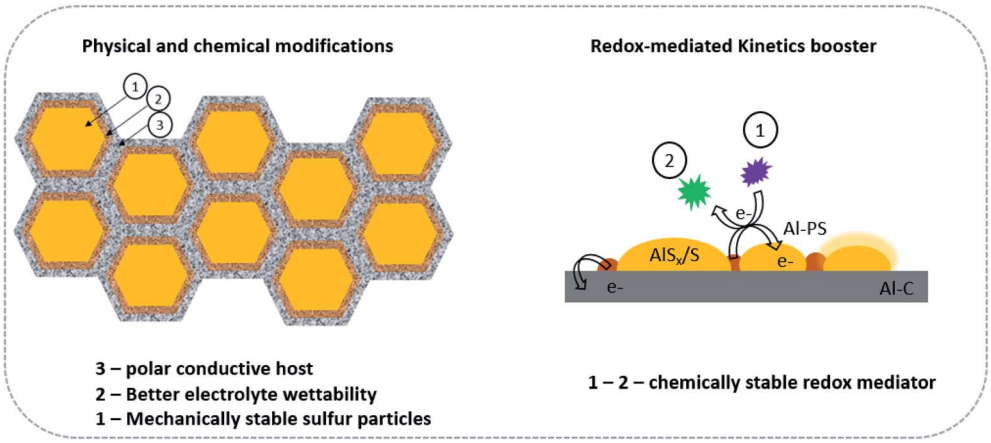

Fig. 8 Advancing Al–S batteries through the design of a next-generation sulfur cathode and introduction of kinetic promoters.

confinement and high chemical adsorption, resulting in improved electrolyte penetration and prevention of diffusion of polysulfide. For instance, a core–shell structure of the sulfur nanospheres@ultrathin δ-MnO_2 composite for Li–S batteries with tailorable high S-mass ratio of 82 weight% was investigated by Li *et al.* (Fig. 9a). The composite showed a remarkable specific capacity of about 846 mA h g^{-1} at 1C with an areal capacity of 502 mA h cm^{-2} @ 1 mA h cm^{-2}.[101] Another group

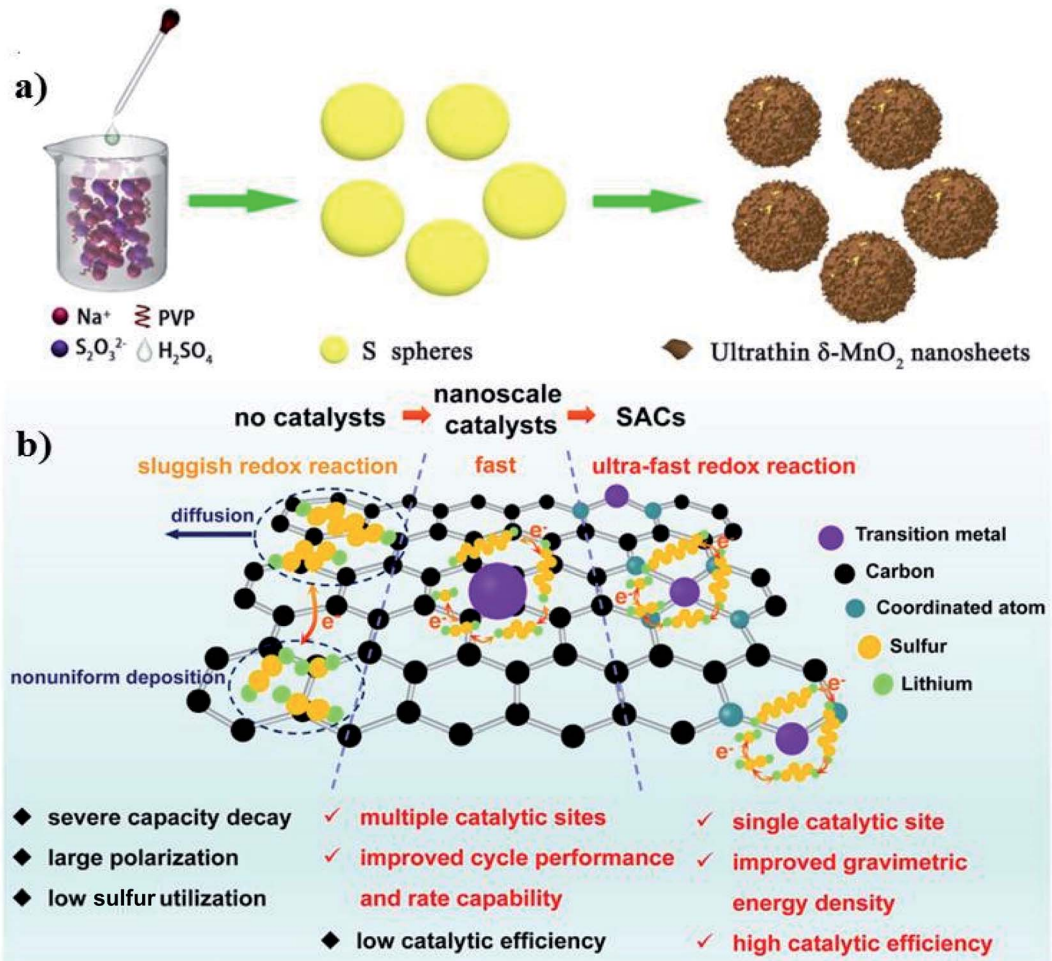

Fig. 9 (a) Schematic illustration for the synthesis of sulfur nanospheres and sulfur nanospheres@ultrathin δ-MnO_2 nanosheet core–shell structures, and the conversion of Li_2S_x on the core–shell surface.[101] Reproduced with permission. Copyright 2020 American Chemical Society. (b) Catalytic mechanism of SACs for sulfur electrodes.[102] Reproduced with permission. Copyright 2021 Elsevier.

(Xiao Liang and Linda) worked on the *in situ* reaction assembly of the core–shell sulfur–MnO_2 cathode of the Li–S battery, where the low capacity fading of 0.039% per cycle for over 1700 cycles was achieved.[100] We expect to achieve similar landmarks. However, the complex reaction chemistry, due to the trivalent nature of Al^{3+}, demands more extensive research on the cathode, anode, and electrolyte separately.

To further boost the redox kinetics of the sulfur conversion, there has been a recent review by the Xiao group in the introduction of single-atom catalysts (SACs) into metal–sulfur batteries.[102] Recently, single-atom catalysts have gained broad interest due to their interactions in accelerating the transfer of charge between the catalysts and substrates. SACs can further reduce the polarization and mitigate the shuttle effect by accelerating the sulfur conversion mechanisms (Fig. 9b). In 2020, Wang *et al.* studied an iron single-atom catalyst anchored on a nitrogen-rich metal–organic framework (MOF) to accelerate the conversion mechanism of the sulfur cathode.[103] Their fabricated FeSA–CN/S composites exhibited low capacity decay of 0.06% per cycle for 500 cycles at 4C, owing to its confined porous monocage-like structure. The high charge density of Al provides hindrances in the efficiency of the battery, which altogether slows down the reaction kinetics of the sulfur cathode. The introduction of SACs into the Al–S batteries can enhance the sluggishness of the cell due to their high catalytic efficiency. In the future, more efforts are expected towards the development of SACs. Thus, its mechanisms can therefore be further explored. Covalent-organic frameworks have been also considered as an advanced electrode material for lithium-ion and sodium ion batteries[104,105] due to their highly featured "structural diversity, framework tenability and functional versatility". They can be constructed *via* incorporation of redox-active sites or units into a porous organic framework to enhance the storage capacity.[106] Owing to the rich-physiochemical properties of the covalent-organic frameworks, they could be served as the potential host for elemental sulfur in the Al–S battery. Other possible solutions to enrich the cathode's performance may include the addition of polyimide particles,[107] organic-based electrode materials[108,109] or nitrogen dopants[110] as the suitable host for the Al–S battery system. In addition, efforts can be made towards the incorporation of metal sulfides or other components with the core–shell architecture to developing favourable cathodic materials for a feasible Al–S battery system.[20,25,26,111]

The development of Al–S batteries with high electrochemical cyclic stability can be explored and carried forward to the next-generation battery system. Even with all these efforts towards this system, the research on Al–S still has a long way to reach its practicality. We believe that our proposed mini-review can influence the research to contribute more towards understanding the cathodic system in Al–S batteries.

Conflicts of interest

There are no conflicts to declare.

Acknowledgements

Sungjemmenla and Chhail Bihari Soni acknowledge the scholarship awarded by the Indian Institute of Technology Delhi (IIT Delhi). This work was financially supported by the IIT Delhi.

References

1 Y. Liang, C. Z. Zhao, H. Yuan, Y. Chen, W. Zhang, J. Q. Huang, D. Yu, Y. Liu, M. M. Titirici and Y. L. Chueh, *InfoMat*, 2019, **1**, 6–32.
2 J. B. Goodenough and Y. Kim, *Chem. Mater.*, 2010, **22**, 587–603.
3 D. Deng, M. G. Kim, J. Y. Lee and J. Cho, *Energy Environ. Sci.*, 2009, **2**, 818–837.
4 M. Armand and J.-M. Tarascon, *Nature*, 2008, **451**, 652–657.
5 D. Larcher and J.-M. Tarascon, *Nat. Chem.*, 2015, **7**, 19–29.
6 E. C. Evart, *Nature*, 2015, **526**, S93.
7 A. Manthiram, *J. Phys. Chem. Lett.*, 2011, **2**, 176–184.
8 A. Manthiram, X. Yu and S. Wang, *Nat. Rev. Mater.*, 2017, **2**, 1–16.
9 H. Jin, S. Xin, C. Chuang, W. Li, H. Wang, J. Zhu, H. Xie, T. Zhang, Y. Wan and Z. Qi, *Science*, 2020, **370**, 192–197.
10 M. H. Braga, N. S. Grundish, A. J. Murchison and J. B. Goodenough, *Energy Environ. Sci.*, 2017, **10**, 331–336.
11 H. Xu, P.-H. Chien, J. Shi, Y. Li, N. Wu, Y. Liu, Y.-Y. Hu and J. B. Goodenough, *Proc. Natl. Acad. Sci. U. S. A.*, 2019, **116**, 18815–18821.
12 K. Zhu, C. Wang, Z. Chi, F. Ke, Y. Yang, A. Wang, W. Wang and L. Miao, *Front. Energy Res.*, 2019, **7**, 1.
13 U. Ulissi, S. Ito, S. M. Hosseini, A. Varzi, Y. Aihara and S. Passerini, *Adv. Energy Mater.*, 2018, **8**, 1801462.
14 Z. W. Seh, Y. Sun, Q. Zhang and Y. Cui, *Chem. Soc. Rev.*, 2016, **45**, 5605–5634.
15 A. Manthiram, S. H. Chung and C. Zu, *Adv. Mater.*, 2015, **27**, 1980–2006.
16 D. Lv, J. Zheng, Q. Li, X. Xie, S. Ferrara, Z. Nie, L. B. Mehdi, N. D. Browning, J. G. Zhang, G. L. Graff, J. Liu and J. Xiao, *Adv. Energy Mater.*, 2015, **5**, 1402290.
17 X. B. Cheng, R. Zhang, C. Z. Zhao, F. Wei, J. G. Zhang and Q. Zhang, *Adv. Sci.*, 2016, **3**, 1500213.
18 W. Hua, Z. Yang, H. Nie, Z. Li, J. Yang, Z. Guo, C. Ruan, X. a. Chen and S. Huang, *ACS Nano*, 2017, **11**, 2209–2218.
19 H. Pan, J. Chen, R. Cao, V. Murugesan, N. N. Rajput, K. S. Han, K. Persson, L. Estevez, M. H. Engelhard and J.-G. Zhang, *Nat. Energy*, 2017, **2**, 813–820.
20 M. Ue, K. Sakaushi and K. Uosaki, *Mater. Horiz.*, 2020, **7**, 1937–1954.
21 L. A. Ellingsen, A. Holland, J. F. Drillet, W. Peters, M. Eckert, C. Concepcion, O. Ruiz, J. F. Colin, E. Knipping, Q. Pan, R. G. A. Wills and G. Majeau-Bettez, *Materials*, 2018, **11**, 936.
22 H. Chen, H. Xu, B. Zheng, S. Wang, T. Huang, F. Guo, W. Gao and C. Gao, *ACS Appl. Mater. Interfaces*, 2017, **9**, 22628–22634.
23 J. Auborn and Y. Barberio, *J. Electrochem. Soc.*, 1985, **132**, 598.

24 Z. Hu, Y. Guo, H. Jin, H. Ji and L.-J. Wan, *Chem. Commun.*, 2020, **56**, 2023–2026.
25 D. Yuan, J. Zhao, W. Manalastas Jr, S. Kumar and M. Srinivasan, *Nano Mater. Sci.*, 2020, **2**, 248–263.
26 T. Leisegang, F. Meutzner, M. Zschornak, W. Münchgesang, R. Schmid, T. Nestler, R. A. Eremin, A. A. Kabanov, V. A. Blatov and D. C. Meyer, *Front. Chem.*, 2019, **7**, 268.
27 J. Muldoon, C. B. Bucur and T. Gregory, *Chem. Rev.*, 2014, **114**, 11683–11720.
28 S. K. Das, S. Mahapatra and H. Lahan, *J. Mater. Chem. A*, 2017, **5**, 6347–6367.
29 Y. Pan, S. Li, M. Yin and J. Li, *Energy Technol.*, 2019, **7**, 1900164.
30 S. Licht, *J. Electrochem. Soc.*, 1997, **144**, L133.
31 G. Cohn, L. Ma and L. A. Archer, *J. Power Sources*, 2015, **283**, 416–422.
32 D. Muñoz-Torrero, J. Palma, R. Marcilla and E. Ventosa, *Dalton Trans.*, 2019, **48**, 9906–9911.
33 S. Wang, Z. Yu, J. Tu, J. Wang, D. Tian, Y. Liu and S. Jiao, *Adv. Energy Mater.*, 2016, **6**, 1600137.
34 K. Xu and A. von Wald Cresce, *J. Mater. Res.*, 2012, **27**, 2327.
35 H. Yang, L. Yin, J. Liang, Z. Sun, Y. Wang, H. Li, K. He, L. Ma, Z. Peng and S. Qiu, *Angew. Chem.*, 2018, **130**, 1916–1920.
36 T. Jiang, M. C. Brym, G. Dubé, A. Lasia and G. Brisard, *Surf. Coat. Technol.*, 2006, **201**, 10–18.
37 W. Simka, D. Puszczyk and G. Nawrat, *Electrochim. Acta*, 2009, **54**, 5307–5319.
38 Z. Akdeniz and M. Tosi, *Z. Naturforsch., A: Phys. Sci.*, 1999, **54**, 180–186.
39 S. Xia, X.-M. Zhang, K. Huang, Y.-L. Chen and Y.-T. Wu, *J. Electroanal. Chem.*, 2015, **757**, 167–175.
40 S. Licht and D. Peramunage, *J. Electrochem. Soc.*, 1993, **140**, L4.
41 M.-C. Lin, M. Gong, B. Lu, Y. Wu, D.-Y. Wang, M. Guan, M. Angell, C. Chen, J. Yang and B.-J. Hwang, *Nature*, 2015, **520**, 324–328.
42 G. A. Elia, N. A. Kyeremateng, K. Marquardt and R. Hahn, *Batteries Supercaps*, 2019, **2**, 83–90.
43 W. Wang, B. Jiang, W. Xiong, H. Sun, Z. Lin, L. Hu, J. Tu, J. Hou, H. Zhu and S. Jiao, *Sci. Rep.*, 2013, **3**, 1–6.
44 A. M. Diem, B. Fenk, J. Bill and Z. Burghard, *Nanomaterials*, 2020, **10**, 247.
45 S. Liu, J. Hu, N. Yan, G. Pan, G. Li and X. Gao, *Energy Environ. Sci.*, 2012, **5**, 9743–9746.
46 N. Hudak, *Rechargeable Aluminum Batteries with Conducting Polymers as Active Cathode Materials*, Sandia National Lab. (SNL-NM), Albuquerque, NM (United States), 2014.
47 N. R. Levy and Y. Ein-Eli, *J. Solid State Electrochem.*, 2020, **24**, 2067.
48 X. Yu and A. Manthiram, *Adv. Energy Mater.*, 2017, **7**, 1700561.
49 X. Yu, M. J. Boyer, G. S. Hwang and A. Manthiram, *Chem*, 2018, **4**, 586–598.
50 J. Smajic, S. Wee, F. R. F. Simoes, M. N. Hedhili, N. Wehbe, E. Abou-Hamad and P. M. F. J. Costa, *ACS Appl. Energy Mater.*, 2020, **3**, 6805–6814.
51 X. Yu and A. Manthiram, *Small Methods*, 2017, **1**, 1700217.
52 D. Peramunage, R. Dillon and S. Licht, *J. Power Sources*, 1993, **45**, 311–323.
53 T. Gao, X. Li, X. Wang, J. Hu, F. Han, X. Fan, L. Suo, A. J. Pearse, S. B. Lee, G. W. Rubloff, K. J. Gaskell, M. Noked and C. Wang, *Angew. Chem., Int. Ed. Engl.*, 2016, **55**, 9898–9901.
54 Z. Gong, Q. Wu, F. Wang, X. Li, X. Fan, H. Yang and Z. Luo, *RSC Adv.*, 2016, **6**, 37443–37451.
55 S. Rehman, K. Khan, Y. Zhao and Y. Hou, *J. Mater. Chem. A*, 2017, **5**, 3014–3038.
56 H. Yang, L. Yin, J. Liang, Z. Sun, Y. Wang, H. Li, K. He, L. Ma, Z. Peng, S. Qiu, C. Sun, H. M. Cheng and F. Li, *Angew. Chem., Int. Ed. Engl.*, 2018, **57**, 1898–1902.
57 Y. Guo, H. Jin, Z. Qi, Z. Hu, H. Ji and L.-J. Wan, *Adv. Funct. Mater.*, 2019, **29**, 1807676.
58 J. Song, M. L. Gordin, T. Xu, S. Chen, Z. Yu, H. Sohn, J. Lu, Y. Ren, Y. Duan and D. Wang, *Angew. Chem., Int. Ed. Engl.*, 2015, **54**, 4325–4329.
59 Y.-L. Ding, P. Kopold, K. Hahn, P. A. van Aken, J. Maier and Y. Yu, *Adv. Funct. Mater.*, 2016, **26**, 1112–1119.
60 Z. Zhang, L.-L. Kong, S. Liu, G.-R. Li and X.-P. Gao, *Adv. Energy Mater.*, 2017, **7**, 1602543.
61 L. Qie and A. Manthiram, *Adv. Mater.*, 2015, **27**, 1694–1700.
62 H. Xu and A. Manthiram, *Nano Energy*, 2017, **33**, 124–129.
63 X. Yu and A. Manthiram, *Adv. Energy Mater.*, 2017, **7**, 1700561.
64 Q. Pang, D. Kundu and L. F. Nazar, *Mater. Horiz.*, 2016, **3**, 130–136.
65 Q. Zhang, G. Peng, J. P. Mwizerwa, H. Wan, L. Cai, X. Xu and X. Yao, *J. Mater. Chem. A*, 2018, **6**, 12098–12105.
66 Ş. Sörgel, O. Kesten, A. Wengel and T. Sörgel, *Energy Storage Materials*, 2018, **10**, 223–232.
67 Z. Yan, J. Xiao, W. Lai, L. Wang, F. Gebert, Y. Wang, Q. Gu, H. Liu, S. L. Chou, H. Liu and S. X. Dou, *Nat. Commun.*, 2019, **10**, 4793.
68 H. Ye, L. Ma, Y. Zhou, L. Wang, N. Han, F. Zhao, J. Deng, T. Wu, Y. Li and J. Lu, *Proc. Natl. Acad. Sci. U. S. A.*, 2017, **114**, 13091–13096.
69 M. L. Meyerson, P. E. Papa, J. A. Weeks, A. G. Paul-Orecchio, A. Heller and C. B. Mullins, *ACS Appl. Energy Mater.*, 2020, **3**, 6121–6126.
70 M. K. Aslam, I. D. Seymour, N. Katyal, S. Li, T. Yang, S. J. Bao, G. Henkelman and M. Xu, *Nat. Commun.*, 2020, **11**, 5242.
71 Z. Yan, J. Xiao, W. Lai, L. Wang, F. Gebert, Y. Wang, Q. Gu, H. Liu, S.-L. Chou, H. Liu and S.-X. Dou, *Nat. Commun.*, 2019, **10**, 4793.
72 J. Balach, J. Linnemann, T. Jaumann and L. Giebeler, *J. Mater. Chem. A*, 2018, **6**, 23127–23168.
73 Y. Lu, X. Li, J. Liang, L. Hu, Y. Zhu and Y. Qian, *Nanoscale*, 2016, **8**, 17616–17622.
74 B. Liu, J. Yang, Y. Han, T. Hu, W. Ren, C. Liu, Y. Ma and C. Gao, *J. Appl. Phys.*, 2011, **109**, 053717.

75 J. M. Falkowski and Y. Surendranath, *ACS Catal.*, 2015, **5**, 3411–3416.
76 X. Liu, J. Q. Huang, Q. Zhang and L. Mai, *Adv. Mater.*, 2017, **29**, 1601759.
77 H. Lin, L. Yang, X. Jiang, G. Li, T. Zhang, Q. Yao, G. W. Zheng and J. Y. Lee, *Energy Environ. Sci.*, 2017, **10**, 1476–1486.
78 H. Tao, M. Zhou, K. Wang, S. Cheng and K. Jiang, *J. Mater. Chem. A*, 2017, **5**, 9322–9328.
79 Z. Zhao-Karger and M. Fichtner, *Front. Chem.*, 2019, **6**, 656.
80 D.-T. Nguyen, R. Horia, A. Y. S. Eng, S.-W. Song and Z. W. Seh, *Mater. Horiz.*, 2020, DOI: 10.1039/D0MH01403F.
81 E. Lancry, E. Levi, Y. Gofer, M. Levi, G. Salitra and D. Aurbach, *Chem. Mater.*, 2004, **16**, 2832–2838.
82 L. Geng, G. Lv, X. Xing and J. Guo, *Chem. Mater.*, 2015, **27**, 4926–4929.
83 J. B. Parise, *Acta Crystallogr.*, 1980, **36**, 1179–1180.
84 H. Gamsjäger, J. Bugajski and W. Preis, *Chemical thermodynamics of nickel*, Elsevier, Amsterdam, 2005.
85 H. Li, H. Yang, Z. Sun, Y. Shi, H.-M. Cheng and F. Li, *Nano energy*, 2019, **56**, 100–108.
86 Z. Yu, Z. Kang, Z. Hu, J. Lu, Z. Zhou and S. Jiao, *Chem. Commun.*, 2016, **52**, 10427–10430.
87 X. Zheng, R. Tang, Y. Zhang, L. Ma, X. Wang, Y. Dong, G. Kong and L. Wei, *Sustainable Energy Fuels*, 2020, **4**, 1630–1641.
88 K. Zhang, T. H. Lee, J. H. Cha, R. S. Varma, J. W. Choi, H. W. Jang and M. Shokouhimehr, *Sci. Rep.*, 2019, **9**, 13573.
89 H. Sohn, M. L. Gordin, M. Regula, D. H. Kim, Y. S. Jung, J. Song and D. Wang, *J. Power Sources*, 2016, **302**, 70–78.
90 J. W. To, Z. Chen, H. Yao, J. He, K. Kim, H. H. Chou, L. Pan, J. Wilcox, Y. Cui and Z. Bao, *ACS Cent. Sci.*, 2015, **1**, 68–76.
91 M. Wang, W. Wang, A. Wang, K. Yuan, L. Miao, X. Zhang, Y. Huang, Z. Yu and J. Qiu, *Chem. Commun.*, 2013, **49**, 10263–10265.
92 J. Wang, J. Yang, Y. Nuli and R. Holze, *Electrochem. Commun.*, 2007, **9**, 31–34.
93 I. Kim, C. H. Kim, S. h. Choi, J.-P. Ahn, J.-H. Ahn, K.-W. Kim, E. J. Cairns and H.-J. Ahn, *J. Power Sources*, 2016, **307**, 31–37.
94 Z.-Q. Jin, Y.-G. Liu, W.-K. Wang, A.-B. Wang, B.-W. Hu, M. Shen, T. Gao, P.-C. Zhao and Y.-S. Yang, *Energy Storage Materials*, 2018, **14**, 272–278.
95 H. M. Kim, J.-Y. Hwang, D. Aurbach and Y.-K. Sun, *J. Phys. Chem. Lett.*, 2017, **8**, 5331–5337.
96 R. Kumar, J. Liu, J.-Y. Hwang and Y.-K. Sun, *J. Mater. Chem. A*, 2018, **6**, 11582–11605.
97 J. Wang, Y.-S. He and J. Yang, *Adv. Mater.*, 2015, **27**, 569–575.
98 W. Wang, Z. Cao, G. A. Elia, Y. Wu, W. Wahyudi, E. Abou-Hamad, A.-H. Emwas, L. Cavallo, L.-J. Li and J. Ming, *ACS Energy Lett.*, 2018, **3**, 2899–2907.
99 M. Zhao, B.-Q. Li, X.-Q. Zhang, J.-Q. Huang and Q. Zhang, *ACS Cent. Sci.*, 2020, **6**, 1095–1104.
100 X. Liang and L. F. Nazar, *ACS Nano*, 2016, **10**, 4192–4198.
101 Q. Li, Z. Ma, J. Li, Z. Liu, L. Fan, X. Qin and G. Shao, *ACS Appl. Mater. Interfaces*, 2020, **12**, 35049–35057.
102 R. Xiao, K. Chen, X. Zhang, Z. Yang, G. Hu, Z. Sun, H.-M. Cheng and F. Li, *J. Energy Chem.*, 2021, **54**, 452–466.
103 C. Wang, H. Song, C. Yu, Z. Ullah, Z. Guan, R. Chu, Y. Zhang, L. Zhao, Q. Li and L. Liu, *J. Mater. Chem. A*, 2020, **8**, 3421–3430.
104 K. Sakaushi, E. Hosono, G. Nickerl, T. Gemming, H. Zhou, S. Kaskel and J. Eckert, *Nat. Commun.*, 2013, **4**, 1–7.
105 K. Sakaushi, G. Nickerl, F. M. Wisser, D. Nishio-Hamane, E. Hosono, H. Zhou, S. Kaskel and J. Eckert, *Angew. Chem., Int. Ed.*, 2012, **51**, 7850–7854.
106 T. Sun, J. Xie, W. Guo, D. S. Li and Q. Zhang, *Adv. Energy Mater.*, 2020, **10**, 1904199.
107 P.-Y. Gu, Y. Zhao, J. Xie, N. Binte Ali, L. Nie, Z. J. Xu and Q. Zhang, *ACS Appl. Mater. Interfaces*, 2016, **8**, 7464–7470.
108 J. Xie and Q. Zhang, *Mater. Today Energy*, 2020, **18**, 100547.
109 J. Xie, Z. Wang, Z. J. Xu and Q. Zhang, *Adv. Energy Mater.*, 2018, **8**, 1703509.
110 Z.-Q. Lin, J. Xie, B.-W. Zhang, J.-W. Li, J. Weng, R.-B. Song, X. Huang, H. Zhang, H. Li and Y. Liu, *Nano Energy*, 2017, **41**, 117–127.
111 G. A. Elia, K. Marquardt, K. Hoeppner, S. Fantini, R. Lin, E. Knipping, W. Peters, J. F. Drillet, S. Passerini and R. Hahn, *Adv. Mater.*, 2016, **28**, 7564–7579.